El-Kherbawy *et al.*
Journal of Engineering and Applied Science (2023) 70:149
https://doi.org/10.1186/s44147-023-00328-z

Journal of Engineering and Applied Science

RESEARCH Open Access

Flexural performance of T-shape light-weight concrete filled steel tubular girder

Mohamed Emam El-Kherbawy[1*], Alaa M. Morsy[1], Maheeb Abdel-Ghaffar[2] and Yasser A. Khalifa[3]

*Correspondence: Mohammedemam300@gmail.com

[1] Arab Academy for Science, Technology and Maritime Transport, Cairo, Egypt
[2] Structural Engineering Department, Cairo University, Cairo, Egypt
[3] Department of Civil Engineering, Military Technical College, Cairo, Egypt

Abstract

This paper proposes an optimization study for both structure and materials to obtain an affordable, long-span, light-weight, and fast-constructing T-shape lightweight concrete-filled steel tubular (LWCFST) girder in order to be used in bridge construction. This research was performed on a hollow steel tube of Steel-52 (yield limit 360 MPa), which was filled with LWC. A set of parameters had been investigated to illustrate its effect on T-shape LWCFST girder stiffness, toughness, resilience, and ultimate carrying load capacity in order to obtain an equivalent stiffness to that of the typically used precast concrete girder. Based on design codes (EN 1994-1-1/Euro code 4 and ANSI/AISC 360-10) that permit the use of LWC as a filler material, the parameters considered were: the thickness of the steel tube, compressive strength of the filler concrete, and the bond condition between the steel tube and filler lightweight concrete. The yielding and ultimate bending capacity were determined based on the interpreted failure criteria of T-shape LWCFST girder, considering non-linear analysis for both material and loads using ANSYSWORKBENCH software. The results showed that T-shape LWCFST girder can be employed as a significant relative economic alternative to a typical precast girder in the bridge construction field, thanks to its high stiffness/weight ratio. The lightweight concrete inside was effectively employed to delay the local web buckling of the steel tube to increase its bending capacity. In addition, it reduced the total self-weight of the bridge's superstructure by 20% compared with a typical precast concrete girder. The dominant failure of T-shape LWCFST girders was found in the upper concrete slab due to the compression stress, even though the tensile cracks in the filler concrete occurred after reaching tensile yield stress in the steel tube. Additionally, increasing the value of friction coefficient between steel tube and light-weight concrete up to 0.8 was found to significantly affect the girder stiffness and has a slight effect after, no matter how high it is.

Keywords: Composite girders, Local buckling, Lightweight concrete, Flexural strength, Light-weight concrete-filled steel tubes, Bond strength, Resilience, Toughness, Yielding carrying load capacity, Ultimate carrying load capacity

Introduction

Nowadays, the trend in civil engineering is the innovation of new high strength with light self-weight construction and building materials. Lightweight concrete (LWC) provides significant light self-weight, proper compressive strength, and a moderate ductile behavior especially when it is used as a filler material in composite structures

[1–5]. Lightweight concrete is a promising material for use especially in hot areas, due to its heat insulation propriety as well as its participation in enhancing both the environment and energy efficiency especially when it is used as a construction material [5, 6]. Lightweight concrete will be extremely effective in infrastructures especially in bridge construction in weak soils and seismic zones [7], thanks to its lightweight and its ease of use in structural elements such as lightweight concrete-filled steel tubular beams and columns. The composite actions between lightweight concrete and steel tube help to delay the local buckling of the steel tube, leading to increasing its carrying load capacity. It is worth mentioning that, the production cost of lightweight concrete is higher than normal concrete, but its lightweight property helps in reducing the concrete dimension of the whole structure and the cost of labor is very low, which makes the difference in the structure's total cost almost equal as well as its fast construction property, which is preferred in fast-tracking projects [8–12].

The bond behavior between LWC and steel is very important in providing significant composite action in lightweight concrete-filled steel tubular beams (LWCFST), which significantly affects the stress distribution between steel and concrete [13, 14]. The effect of using lightweight fiber-reinforced concrete was discussed by Campione et al. [15] who focused on the local bond stress of the reinforcement bars with LWC and its slippage behavior and found that LWC showed a significant bond behavior under cyclic loads, in addition to a better post peak ductile behavior thanks to fiber reinforcement. Bahrami et al. [16] presented the effect of using wasted rock wool with lightweight concrete on the bond behavior with steel tubes after exposure to high temperatures. The results concluded that using rock wool in the concrete mix increased the bond behavior at 200 °C and 400 °C by 20.2% and 18.2% respectively.

Many researches were performed to improve LWC strength such as Sikora et al. [17] who found that, partial replacement of cement with nano silica showed a noticeable increase in both LWC compressive and flexural strengths. Chung et al. [18] presented an experimental and numerical investigation of the effectiveness of different types of binder additives such as fly ash, liapor, limestone, and fine sand, on LWC strength showing that binder additives participated in enhancing the mechanical properties of LWC, which in turn increased its compressive strength. Tajra et al. [19] discussed the mechanical properties of LWC with lightweight aggregate cored shell (CSA), which was produced through the cold bonding method and revealed that lightweight CSA concrete was of dry density ranging from 1115 to 1540 kg/m^3 and compressive strength from 17.9 to 29.1 MPa, which is appropriate strength relative to its density. Both the flexural strength of LWCFST and its ductility are dependent on the steel wall thickness, compressive strength of filler LWC, confinement factor, and height/wall thickness of the steel tube.

The failure criteria for CFST beams filled with both LWC and self-compacted concrete (SCC) were also discussed by Al-Shaar and Göğüş [20]. The failure modes were identical and can be summarized as, the local buckling of the compression flange, in addition to cracking of filler concrete and then, fracture of the tension flange at large deflections. Al-Shaar also concluded that the ductility of the hollow steel tube was obviously raised in case of filling it with LWC and SCC. In addition, the ratio between the LWCFST/SCCFST was found as 0.85.

Many design codes are used to determine both stiffness and flexural strength of LWCFST in terms of LWC compressive strength, steel tube wall thickness, friction coefficients between LWC and steel tube, including the American Specification AISC 360–10 [21], Guide to European Code EC4-2004 [22], Chinese Specifications DBJ/T13-51–2010 [23], Australian standard AS 5100.6–2004 [24], and the Japanese standard AIJ-1987 [25]. LWC also showed a great performance in LWCFST beams against impact loads, which showed an acceptable ductile behavior against impact loads as well as keeping LWCFST beam structural integrity [26].

Sifan et al. [27] conducted a comparative study to evaluate the flexural strength of CFST beams filled with LWC and normal mix concrete (NMC). The parametric study was performed using a validated Finite Element Model (FEM) using ABAQUS software. Sifan concluded that LWC had a significant participation in delaying the local buckling of the steel tube and therefore, increasing its bending capacity. In addition, a design guideline was proposed to determine the ultimate moment capacity for LWCFST beams.

Gulec et al. [28] presented the effect of using lightweight concrete with a prefabricated steel cage subjected to flexural loads in terms of ultimate capacity and moment-displacement relationship showing that, the ultimate capacity of LWCFST beams was higher by 38% than the traditionally reinforced steel control beams. In addition, the vertical strip in prefabricated beams kept the structural integrity of the beam.

Sifan et al. [29] showed the shear resistance of the LWCFST beam and developed a simple design guideline through Direct Strength Method (DSM) to determine its shear ultimate capacity. Sifan found that LWC participated in stiffening the steel tube and delaying the local buckling of the steel tube due to shear, which increased both the post-buckling and shear capacity of the LWCFST beam. Uenaka and Mizukoshi [30] presented the performance of LWCFS beams subjected to a four-point loading test in the form of both estimated and experimental bending capacities. The results concluded that the LWCFST beams showed a significant moment capacity at both yielding and ultimate points. Accordingly, it was found also, that the ratios between experimental to estimated bending capacities equal 1.9 and 1.19 upon steel tube both yielding and ultimate points respectively with a great correlation factor (r) equal to 0.99.

AL-Eliwi et al. [31] investigated LWCFST circular columns subjected to axial compression loads in terms of tube Diameter to its thickness ($^{D}/_{t}$) and concluded that, using thinner tubes is preferred for the long columns, which prevents the tube's local buckling and therefore, increases its ductility and compression capacity. In addition, the experimental results had 8% and 10% deviation from the results determined according to AISC360-16 and EC4 specifications respectively.

Based on the aforementioned literature, specifications, and design codes (EN 1994–1-1/Euro code 4 and ANSI/AISC 360–10) that permit using LWC as a filler concrete, this research presents an investigation for a T-shape LWCFST composite girder in terms of toughness, resilience, ductility, and ultimate carrying load capacity. The proposed T-shape LWCFST girder provides a lightweight, high weight/stiffness ratio, and cost-effective alternative to the conventional precast normal concrete girder in bridge construction. T-shape LWCFST girder participated in reducing the total lumped mass on the piers by 20%, which will enhance the performance of the bridges against seismic excitations in seismic zones. It is worth mentioning that, the LWC is more expensive

Table 1 Description of steel tube [33]

Beam type	Specimen size (bxd)	Wall Thickness (t)	($^{d}/_{t}$)	Length (L)	Steel Strength (f_y)	Concrete Strength (f_{cu})
Unit	mm	mm	Ratio	mm	MPa	MPa
B-1	88.9 × 88.9	3.2	27.8	1200	241	N.A
B-2		3.2	27.8	1200	241	26.03
B-3		3.2	27.8	1200	241	24.8

Table 2 Mechanical properties of concrete [33]

Type of concrete	f_{ck}* (MPa)	f_{cr}* (MPa)	f_{ct}*(MPa)
Conventional concrete	26.03	3.16	2.36
Partial replacement of coarse aggregate, with 25% granite	24.8	3.17	2.35

*indicates the average of three cubes, prism, and cylinders respectively

than NMC. However, it is preferred for use because this reduction in weight also helped in reducing the own weight of bridge substructure elements such as piers, pile caps, and piles, reducing the overall budget of bridge construction, making it cost-effective during construction in weak soils.

Validation

Finite element model description

The validation was performed on a 3-D finite element model against the experimental study of Ghannam [32], on three types of CFST beams: B_1, B_2, and B_3. Steel tube was modeled as 3-D solid 185 elements (8 nodes element), while filler concrete was modeled as 3-D solid 65 elements (8 nodes element) for the three types of beams considering that, the filler concrete wasn't provided with any steel reinforcement bars. Both geometric nonlinearity and filler concrete damage were considered in the analysis, by activating the large deflection property in ANSYS WORKBENCH software. This property updated the stiffness of the beam each time step and considered both infinitesimal and finite strains that occurred. Therefore, it took into consideration the failure that occurred in filler concrete and steel tubes. The results were compared with the experimental results of Ghannam [32]. Beam (B_1) represented the hollow steel tube without any filler concrete, while B_2 and B_3 represented the steel hollow tube filled with normal concrete and partially replaced coarse aggregate concrete with granite respectively. Both steel tube description and mechanical properties of filler concrete are provided in Tables 1 and 2 respectively.

ANSYS WORKBENCH software was used in finite element analysis against the experimental work. It is a finite element analysis software, used to perform stress analysis for both the verification (against the experimental work) and for the T-shape LWCFST girder case study, using advanced solver options. These options involved static analysis, material nonlinearity, and geometric nonlinearity.

Both steel tube and filler concrete were of fine uniform mesh sizes of 15 × 15 mm. This mesh size was specified based on a conducted mesh convergence, throughout many iterations carried out by varying the mesh density in successive iterations. This mesh size

Fig. 1 (S.Ghannam) experimental work test specimens [32]

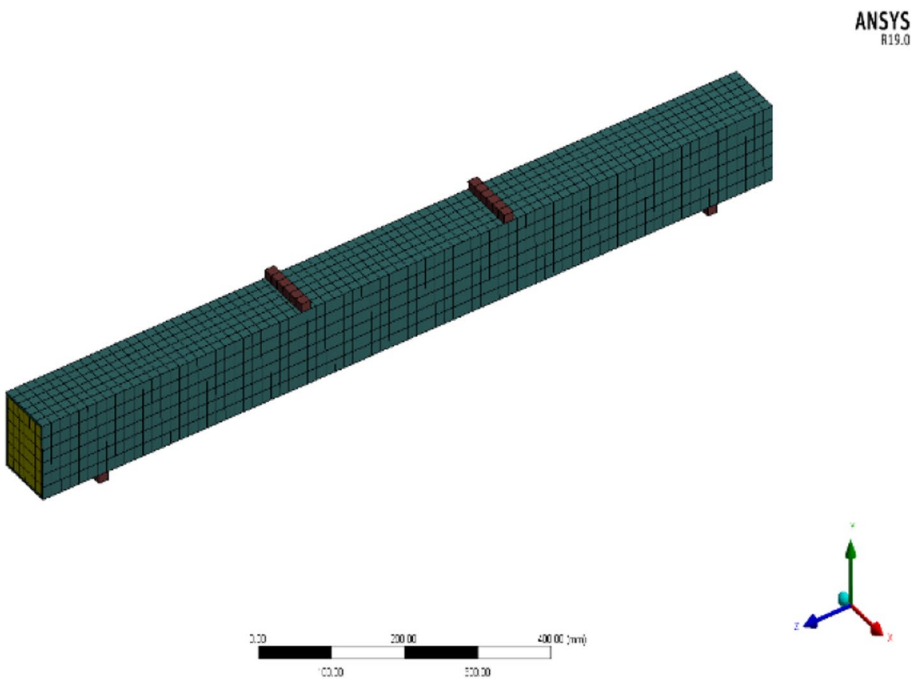

Fig. 2 FEM (15 × 15) mm mesh size

was appropriate enough to get an acceptable accuracy to that of the experimental work. Furthermore, a complete bond type was defined for the contact between steel tube and filler concrete. Figures 1 and 2 [32] represent both experimental work test specimens and FEM-appropriate mesh size respectively.

Materials description of (CFST) beams

Steel and filler concrete were both regarded as bilinear isotropic hardening materials. The constitutive relationships were established automatically using an ANSY WORKBENCH built-in module as shown in Figs. 3 and 4 [33]. The material nonlinearity was defined in terms of material yield strength and the tangent modulus. The tangent

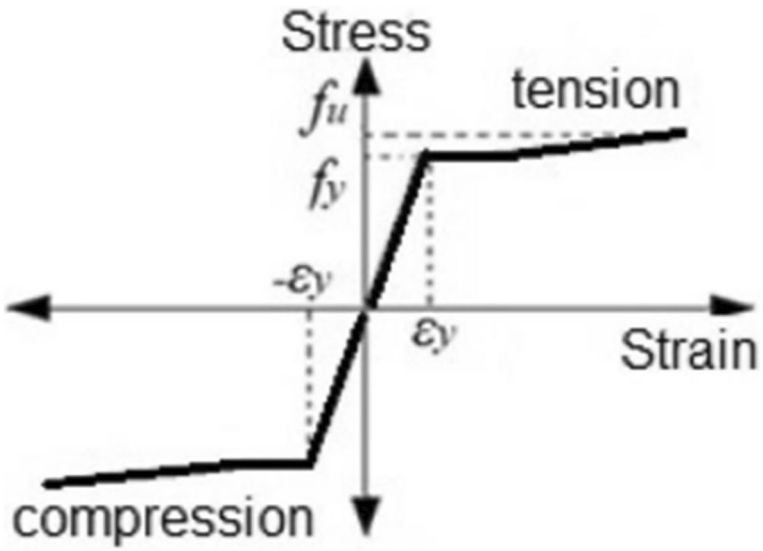

Fig. 3 Steel constitutive relationship [33]

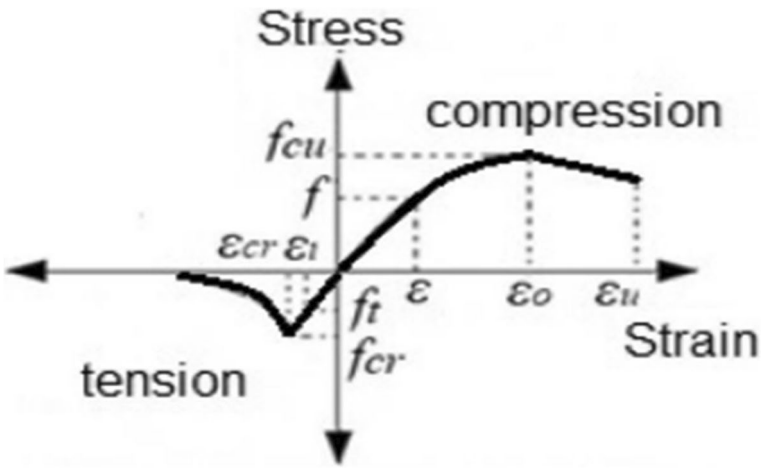

Fig. 4 Concrete constitutive relationship [33]

modulus was considered equal to zero, which makes the materials behave perfectly like plastic.

Analysis of the finite element model

The four-point loading bending test was simulated and analyzed using finite element models for the three types of beams B_1, B_2, and B_3. The beams were supported by two hinged supports of zero displacements at the X, Y, and Z axes, and were free for rotation around the same axes. The applied loads were assigned as two concentrated time stepped point loads ($^{P}/_{2}$), spaced at equal distances of 400 mm from the supports as shown in Fig. 5. In the analysis, eight-time steps with equal intervals of one second were taken into account. Each sample's yielding load capacity was determined by gradually increasing the applied load and recording the corresponding deformations till the

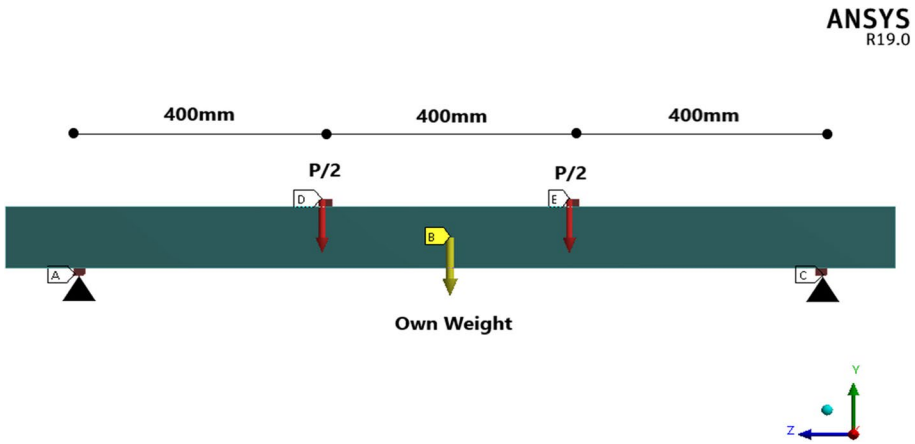

Fig. 5 Four-point loading test setup

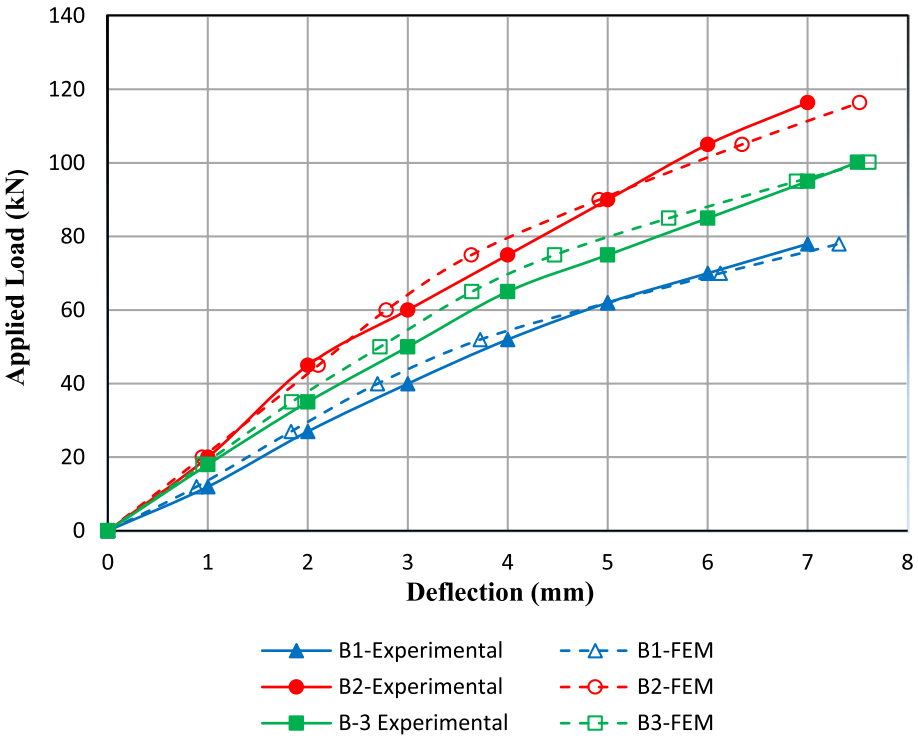

Fig. 6 Load–deflection curves for B1, B2, and B3

yielding of the steel tube. By progressively increasing the load up to complete failure and recording the corresponding deformations, the ultimate load capacity was determined.

The results were collected as the load value described in Ghannam's experimental work and its corresponding displacement for both FEM and experimental work. The data were recorded, plotted, and compared, considering that, the stopping criterion was the last load step mentioned in Ghannam's experimental work.

The results from FEM were convergent to the experimental work by 93.5%, 94%, and 95% for B_1, B_2, and B_3 respectively as shown in Fig. 6. The convergence percentages were calculated as, the average of the results of yielding and ultimate points for each beam.

The convergency percentages were acceptable relative to the number of validated finite element models, and it is worth mentioning that, some minor divergences (less than 7%) were attributed because of the difference in mechanical properties (f_{ck}^{*}, f_{cr}^{*}, and f_{ct}^{*}) for each type of filler concrete.

Methods

Research significance and objective

In this research, an optimization study for both structure and material was performed on a proposed T-shape LWCFST girder to obtain an affordable, long span, light-weight, and fast-constructing girder, in order to be used in bridge construction, especially in extreme seismic zones and weak soils conditions. The girder composed of a hollow steel tube was of steel-52 (yield limit 360MPa) filled with filler concrete of various characteristic cube strengths and specific densities. A set of parameters was investigated in order to obtain an equivalent stiffness to the typical precast concrete girder. The parameters considered were the thickness of the steel tube, the compressive strength of the filler concrete, and the bond condition between the steel tube and filler concrete. These parameters were chosen, based on the design codes and specifications, that permit using LWC, due to their significant influence on the girder stiffness [22, 23]. In this research, the targeted stiffness is referenced and compared to the stiffness of a conventional precast concrete girder, which is currently utilized in many existing bridges in Egypt. Finite element models were established for both Precast concrete and T-shape LWCFST girders using ANSYS WORKBENCH software, considering non-linear analysis for both materials and loads. The results of each parametric study were displayed, in terms of toughness, resilience, and the ultimate carrying load capacity of the girder, revealing its stiffness and ductility.

FEM development for typical precast girder

For a typical precast concrete girder that weighs 1128.4 kN, and is currently utilized in many bridges in Egypt, a FEM was established for a 28,000 mm span girder [34]. The girder rested on elastomeric bearings of $400 \times 500 \times 200$ mm modeled as spring elements having a triaxial stiffness indicated in Table 3 as shown in Figs. 7 and 8. The precast girder was modeled as a solid 65 element (8 nodes element) with 15×15 mm fine meshing size deduced from the validation study. The concrete dimensions of the precast concrete girder are shown in Figs. 9, 10, 11, and 12 [34].

Material model of precast girder

Precast concrete was defined as a bilinear isotropic hardening material. Its stress–strain curve was established automatically using the ANSYS WORKBENCH built-in module

Table 3 Elastomeric bearings stiffness

Stiffness	Value	Unit
X	2000	kN/m
Y	2×10^{6}	kN/m
Z	2000	kN/m

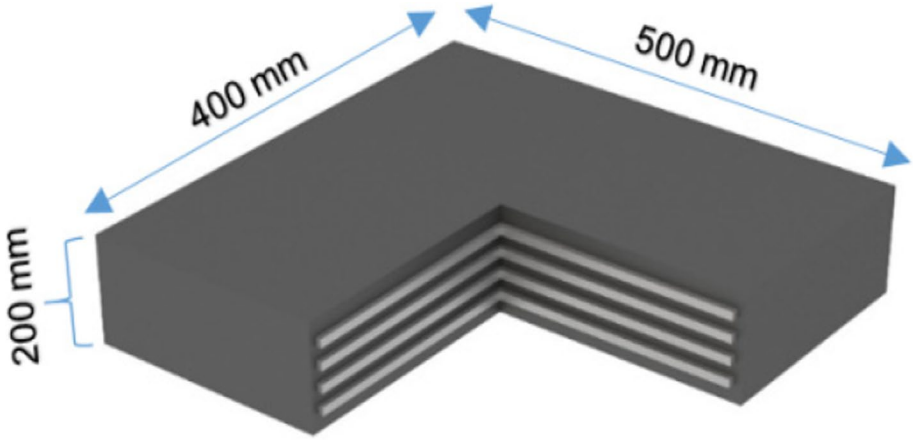

Fig. 7 Elastomeric bearing size

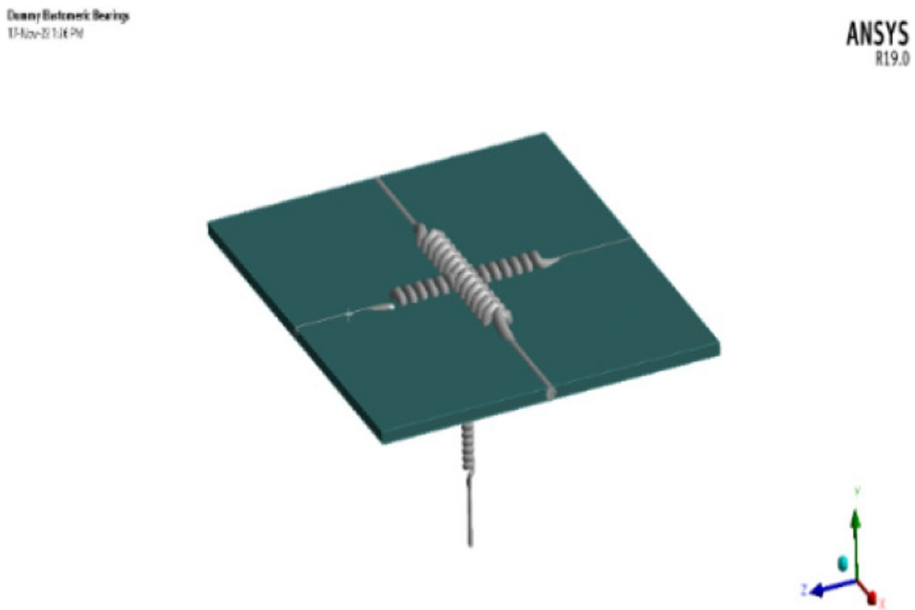

Fig. 8 Elastomeric bearing simulation

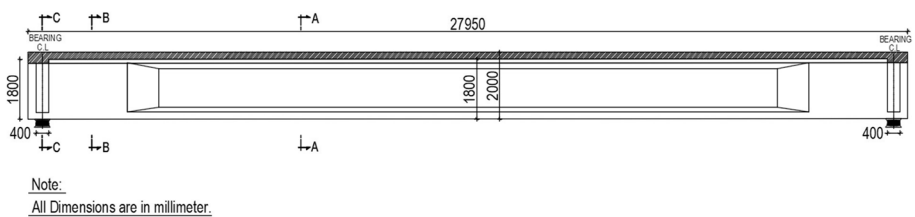

Fig. 9 Precast girder elevation view

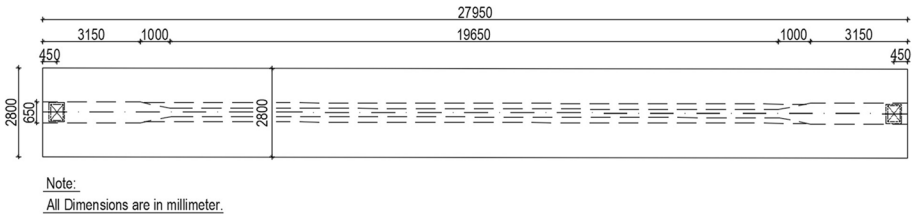

Fig. 10 Precast girder plan view

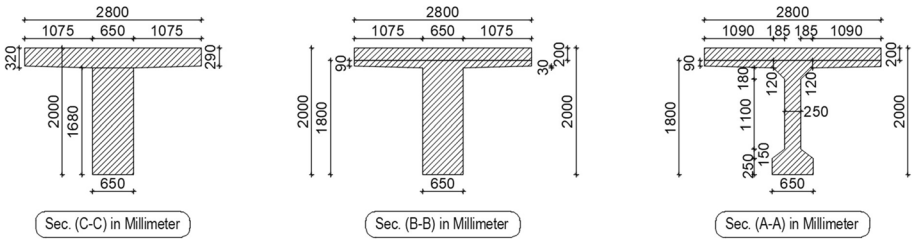

Fig. 11 Precast girder cross sections [34]

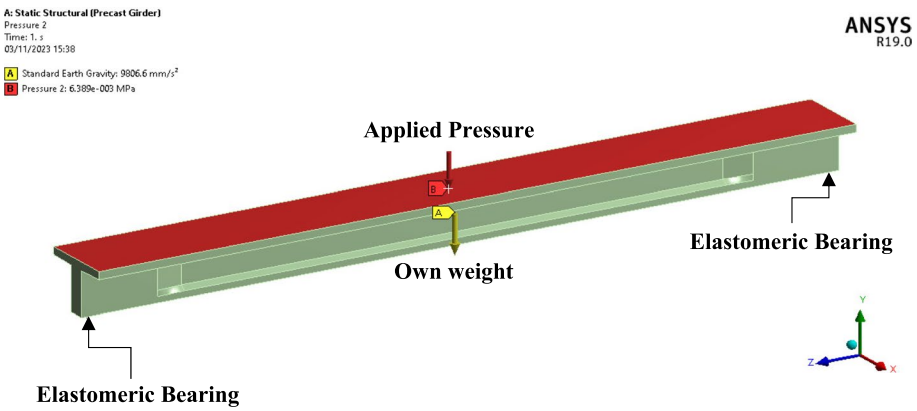

Fig. 12 Modeling of precast girder

in terms of its compressive strength and tangent modulus. The tangent modulus was considered equal to zero, which makes concrete behavior perfectly plastic. The mechanical properties of the concrete are indicated in Table 4.

FEM development for T-shape LWCFST girder

The proposed T-shape LWCFST girder was of 28,000mm span and 2000 mm depth including the concrete slab thickness. The concrete slab was 2800 mm in width and 200 mm in thickness. T-shape LWCFST girder rested on the same aforementioned elastomeric bearings on either side. Shear studs (UPN 160) were also provided, which were spaced equally at 400 mm C/C to prevent sliding of the concrete slab and resist the complementary horizontal shear force due to the girder major-axis bending. Steel tube and shear studs were modeled as 3-D solid 185 elements (8 nodes elements), while filler concrete and concrete slab were modeled as 3-D solid 65 types (8 nodes elements). All

Table 4 Concrete mechanical properties

Property	Value	Unit
Density	25	kN/m^3
Coefficient of thermal expansion	1.5×10^5	C^{-1}
Young's modulus	30511	MPa
Poisson's ratio	0.2	-----
Bulk modulus	1.695×10^4	MPa
Shear modulus	1.271×10^4	MPa
Compressive strength	50	MPa
Tensile strength	5	MPa
Tangent modulus	0	MPa

elements were of fine uniform mesh size of 15×15 mm deduced from the validation study. Moreover, the contact condition between the steel tube and filler concrete was considered as a complete bond type. Figures 13, 14, 15, 16, and 17 illustrate the dimensions of the proposed T-shape LWCFST girder for both steel tube and LWC.

Material models of T-shape LWCFST girder

Steel and filler concrete were both regarded also as bilinear isotropic hardening materials via an ANSY WORKBENCH built-in module in terms of materials yield strength and the tangent modulus. The tangent modulus was considered equal to zero, which makes the materials behave perfectly plastic. The constitutive relationships of the two materials were defined as mentioned in the validation study as shown in Figs. 4 and 5 [33]. The mechanical properties of both steel tube and filler concrete are shown in Tables 5 and 6.

Material models analysis

The materials' non-linearity was analyzed via the ANSYS WORKBENCH built-in module, which automatically determined the stress–strain curves as well as the constitutive relationships between steel and concrete using both the Voce hardening law and the

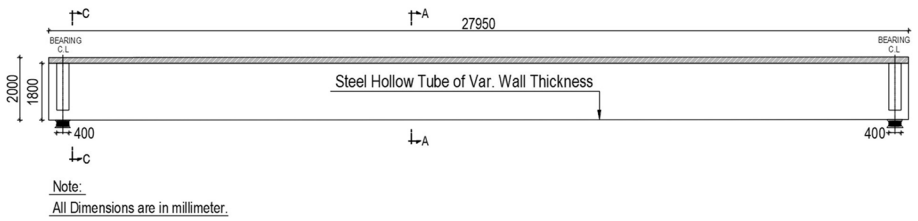

Fig. 13 T-shape LWCFST girder elevation view

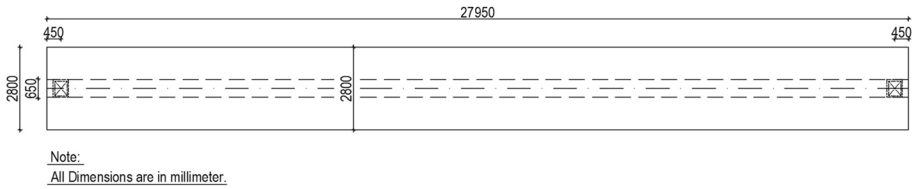

Fig. 14 T-shape LWCFST girder plan view

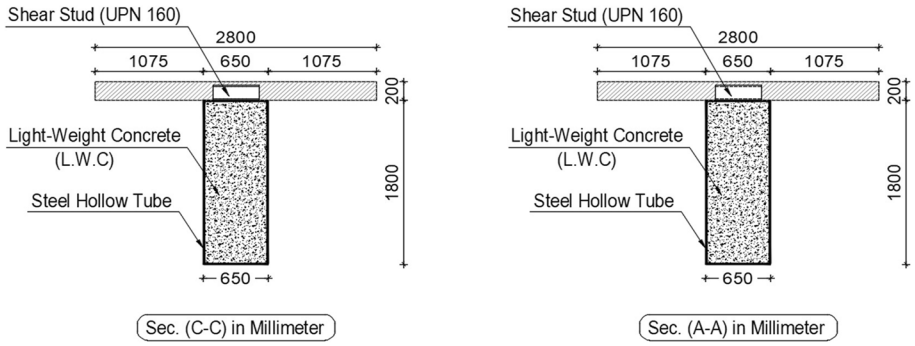

Fig. 15 T-shape LWCFST girder cross-sections

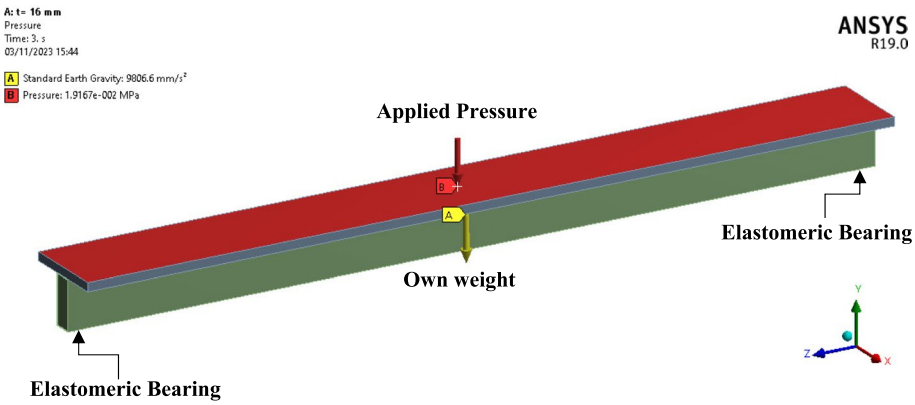

Fig. 16 Modeling of T-shape LWCFST girder

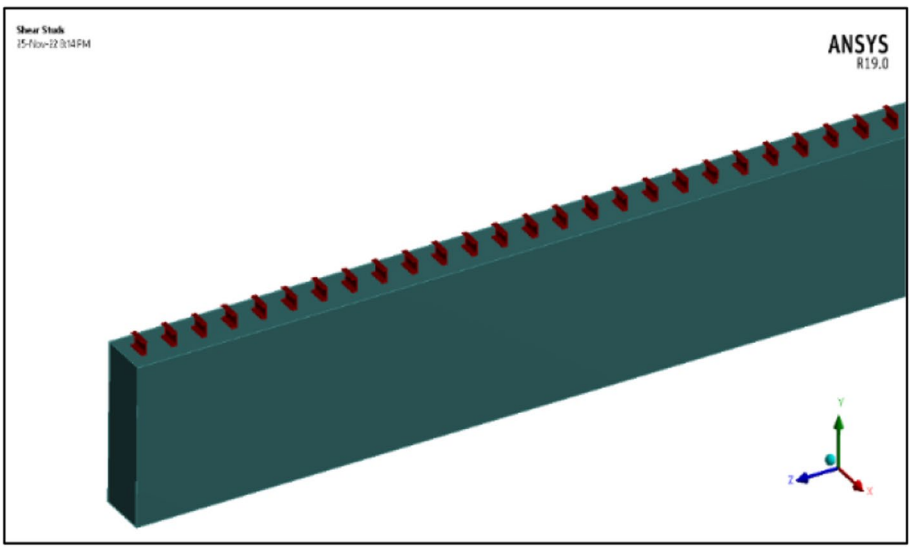

Fig. 17 Shear studs (UPN 160)

Table 5 Mechanical properties of steel-52

Property	Value	Unit
Density	78.50	kN/m^3
Coefficient of thermal expansion	1.2×10^5	C^{-1}
Young's modulus	2.1×10^5	MPa
Poisson's ratio	0.3	-----
Bulk modulus	1.75×10^5	MPa
Shear modulus	8.077×10^4	MPa
Compressive strength	50	MPa
Yield strength	360	MPa
Ultimate strength	520	MPa
Tangent modulus	0	MPa

Table 6 Mechanical properties of lightweight concrete

Property	Value	Unit
Density	6.5	kN/m^3
Coefficient of thermal expansion	1.4×10^5	C^{-1}
Young's modulus	12945	MPa
Poisson's ratio	0.2	-----
Bulk modulus	7.1915×10^3	MPa
Shear modulus	5.3937×10^3	MPa
Compressive strength	9	MPa
Tensile strength	0.9	MPa
Tangent modulus	0	MPa

nonlinear power hardening law [35, 36] in terms of material yield strength and the tangent modulus as follows:

- Non-linear power hardening law [35].

$$\overline{\sigma} = k'\overline{\varepsilon}^{n}\overline{\varepsilon}'^{m} \tag{1}$$

Where k', n and m are three constants of the material, which are the strength coefficient, strain-hardening exponent, and strain rate sensitivity index respectively as shown in Fig. 18 [35].

- Voce law [36].

$$\overline{\sigma} = B - (B - A)\exp(-C\overline{\varepsilon}) \tag{2}$$

Where A, B, and C are material constants used for determining the instability points of extension phases of the material relative to the applied load as shown in Fig. 19 [36].

Girders static structural finite element analysis

Finite Element Analysis (FEA) for both precast and T-shape LWCFST girders was performed using the ANSYS WORKBENCH static structure analysis system, following

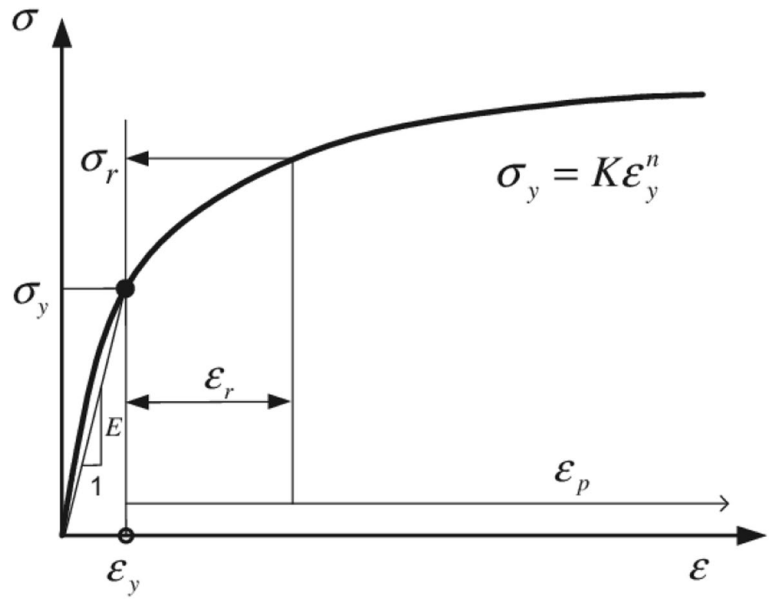

Fig. 18 Stress–strain curve based on power hardening law [35]

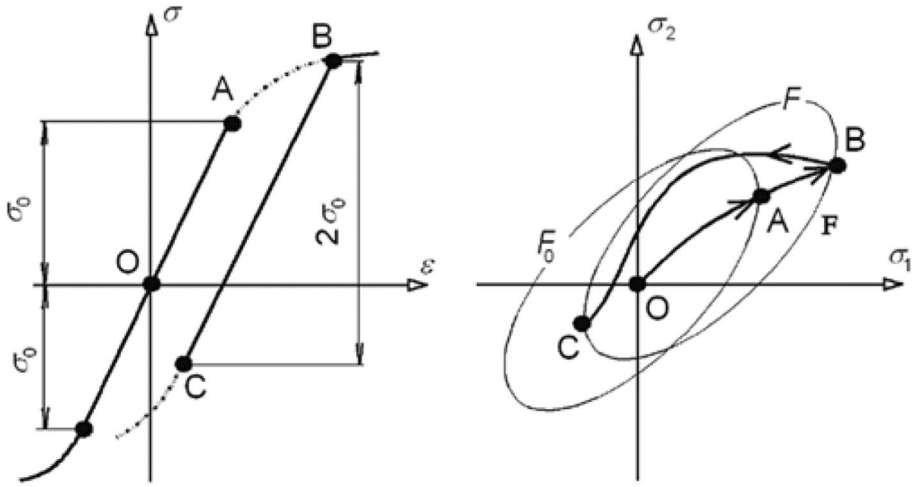

Fig. 19 Stress–strain curve based on Voce law [36]

Dolati and Maleki [37] to perform an accurate FEA. The analysis boundary conditions represented in applied service loads, as well as elastomeric bearings degrees of freedom. The applied loads were the girder's own weight defined as standard gravity load in addition to the applied service live load as shown in Figs. 12 and 16. The service live load was expressed as a time-stepped pressure on the concrete slab. The pressure resultant increased by 500 kN each time step up to complete failure. The elastomeric bearings were considered as partially hinged against displacements in the *X*, *Y*, and *Z* axes with the same stiffness indicated in Table 3 and free for rotation around the *X*, *Y*, and *Z* axes [38].

LWCFST girder parametric studies

Based on the aforementioned specifications and design codes (EN 1994-1-1/Euro code 4 and ANSI/AISC 360-10) that permit using LWC as a filler material, a set of parameters was considered in the analysis, to obtain an equivalent stiffness to the precast concrete girder. The parameters considered were as follows:

- In order to investigate the influence of filler concrete compressive strength on the flexural stiffness of the T-shape CFST girder, as well as identify (f_{cu}) needed for the filler concrete inside the 4mm tube to obtain the same stiffness of the precast girder, eight strengths were studied, such as LWC 9 MPa, 20 MPa, 25 MPa, 30 MPa, 35 MPa, 40 MPa, 45 MPa, and 50 MPa.
- The effect of increasing steel tubular section wall thickness was also studied to investigate its effect on the flexural stiffness of T-shape LWCFST girder and determine the required wall thickness (t_w) accomplishes an equivalent stiffness to the precast girder. Nine wall thicknesses were chosen, based on their availability in the local market in Egypt: 4 mm, 8 mm, 12 mm, 16 mm, 20 mm, 24 mm, 28 mm, 32 mm, and finally 16 mm flange thickness with 4 mm web thickness. The cracking of LWC is not discussed because it was used only as a filler material to delay the local web buckling of steel tube.
- The contact condition between LWC and 4mm steel tube was also investigated because it has a significant effect on T-shape LWCFST girder stiffness. Most designers assume the contact between LWC and steel tubes as a bonded type during the design process. This assumption is not an accurate description, while the bond actually behaves as a friction type [39–41]. The friction contact type was expressed analytically by seven friction coefficients (μ): 0.2, 0.4, 0.6, 0.8, 1.2, 1.4, and 1.6. The friction bond was studied to represent the variation in girder stiffness compared to the complete bond type [27].

Results

The following ANSYS Figures illustrate deformed shapes and normal stresses for both precast and LWCFST girder representing the material nonlinearity via stress contours of material yielding (Figs. 20, 21, 22, 23 and 24).

Filler concrete f_{Cu} a parametric study is expressed as a plotted relationship between applied loads versus the generated deflections. It demonstrates the impact of increasing filler concrete f_{Cu} on T-shape CFST girder stiffness, toughness, resilience, and ultimate carrying load capacity. It also demonstrates that 35 MPa was optimal to accomplish an equal stiffness to the precast concrete girder as shown in Fig. 25.

Steel tube wall thickness (t_w) parametric study is expressed as a plotted relationship between applied loads versus the generated deflections. It demonstrates the impact of increasing the wall thickness of steel tube on T-shape LWCFST girder stiffness, toughness, resilience, and ultimate carrying load capacity. It also demonstrates that 16 mm tube wall thickness was optimal to accomplish an equal stiffness to the precast girder as shown in Fig. 26.

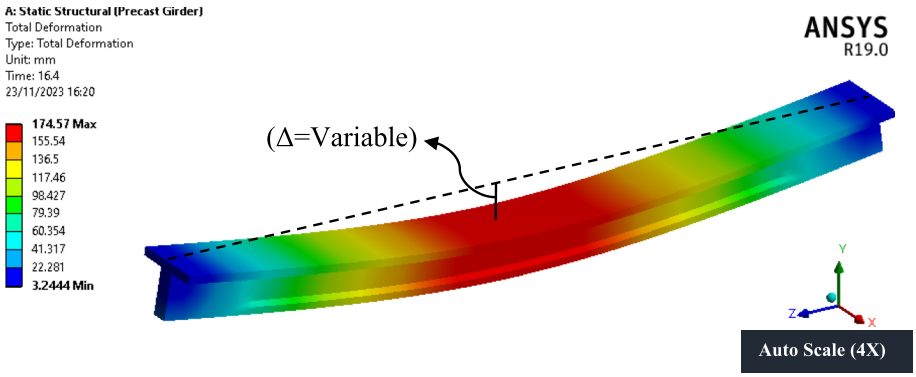

Fig. 20 Precast girder deformed shape

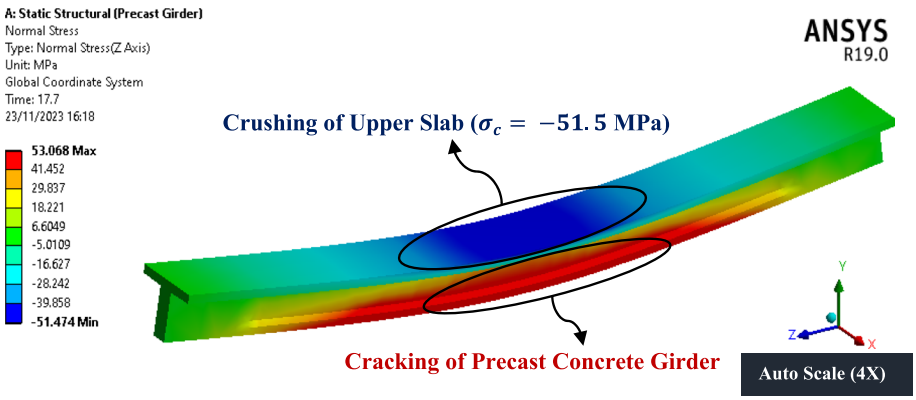

Fig. 21 Precast girder normal stress

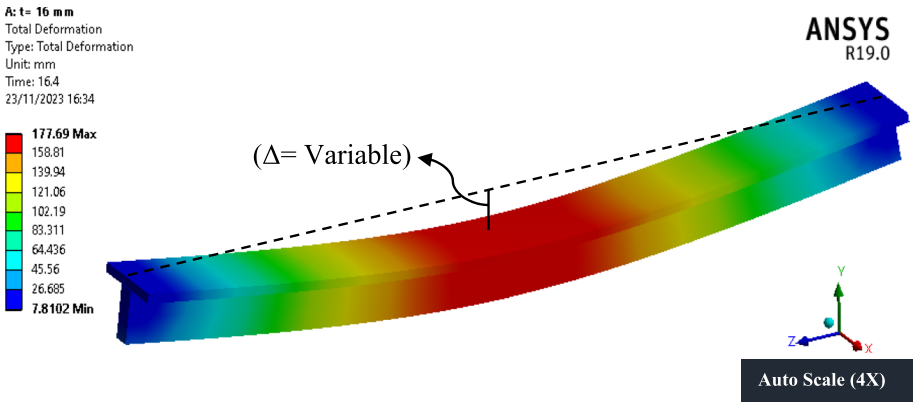

Fig. 22 T-shape LWCFST girder deformed shape

Due to the variation of steel tube wall thickness, the ratio between the tube depth to its wall thickness (d/t) was also a parameter inversely proportional to the ultimate carrying load capacity of the T-shape LWCFST girder. Figure 27 demonstrates the relationship between the ultimate carrying load capacity and the ratio (d/t).

The ultimate carrying load capacity can be determined in terms of (d/t) for T-shape LWCFST girder using the power equation deduced from Fig. 27 as follows:

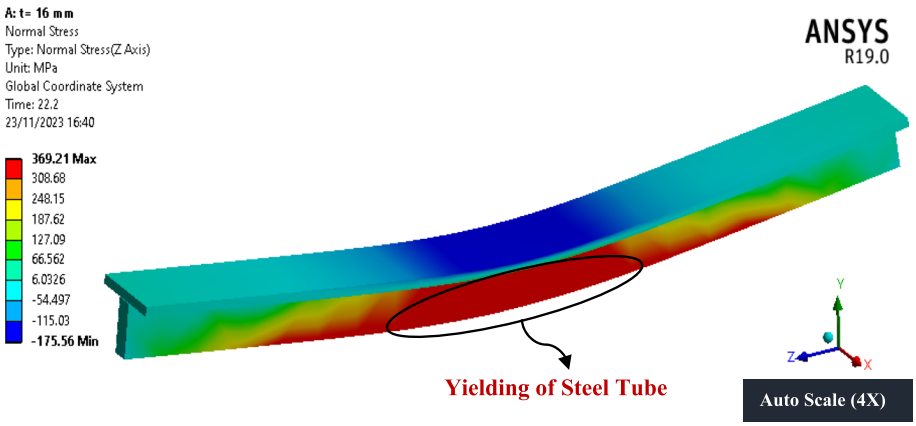

Fig. 23 Normal stress of tube thickness parametric study

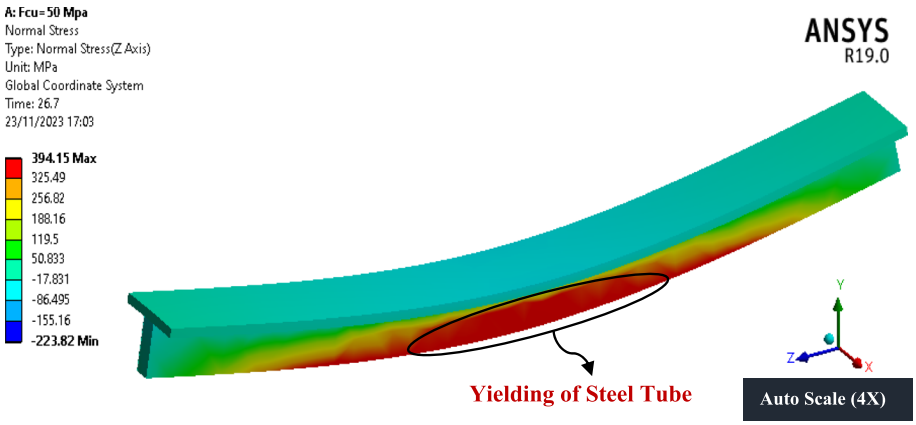

Fig. 24 Normal stress of filler concrete f_{cu} parametric study

$$P_u(kN) = (200085) * (d/t)^{-(0.629)} \tag{3}$$

This equation is valid for $P_u, d, t \in R$, where, $t > 0$ and $P_u \geq 0$.

The friction coefficient (μ) parameter is expressed as a plotted relationship between the applied loads and generated deflections. It demonstrates the impact of considering the contact condition between steel tube and LWC as a friction bond type instead of a complete bond type. In addition, it displays the reduction percentage in T-shape LWCFST girder resilience, toughness, and carrying load capacity at both yield and ultimate points. The impact of composite action between the steel tube and LWC concrete on the girder ductility is also presented by using the steel tube twice with/out lightweight concrete bonding effect as shown in Fig. 28.

Discussion

The parametric study of filler concrete f_{cu} showed that, f_{cu} is directly proportional to the overall stiffness of the CFST girder [42–44]. Increasing filler concrete f_{cu} leads to increasing Young's modulus, which is also in direct proportion to the stiffness according to the following equations.

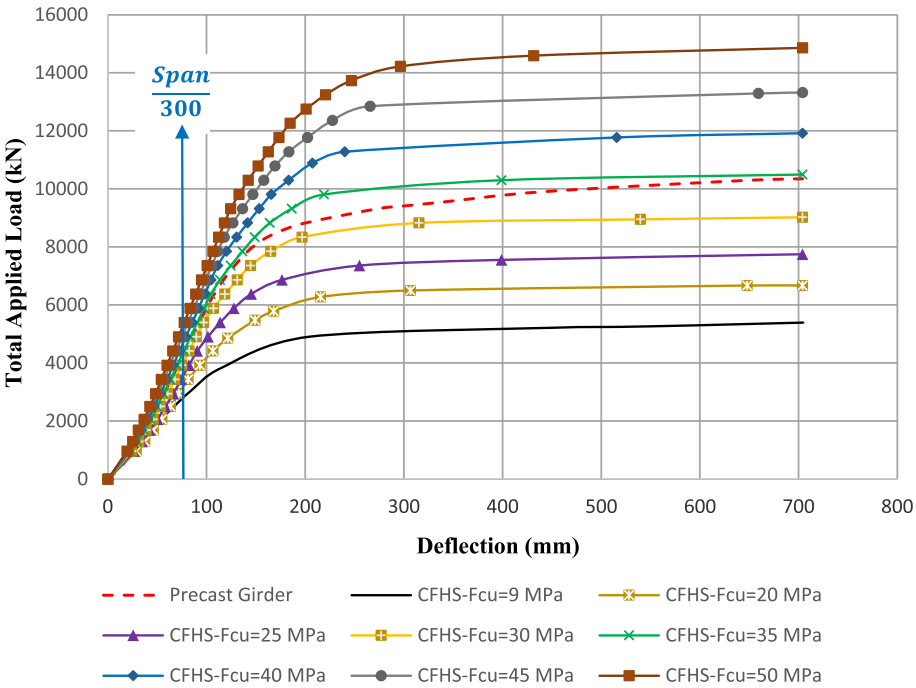

Fig. 25 Stiffness curves for (f_{cu}) parametric study

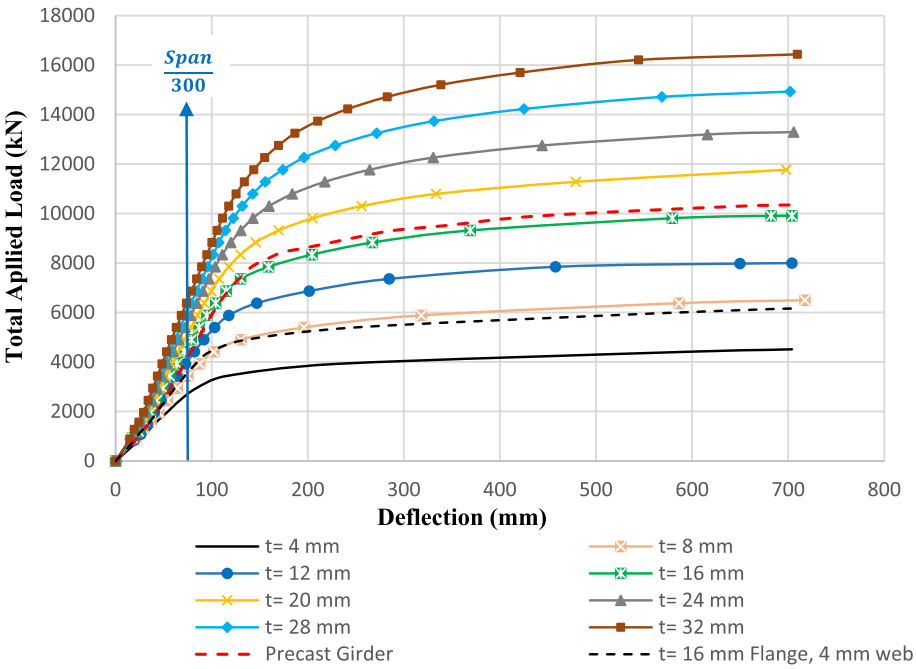

Fig. 26 Stiffness curves (t_w)

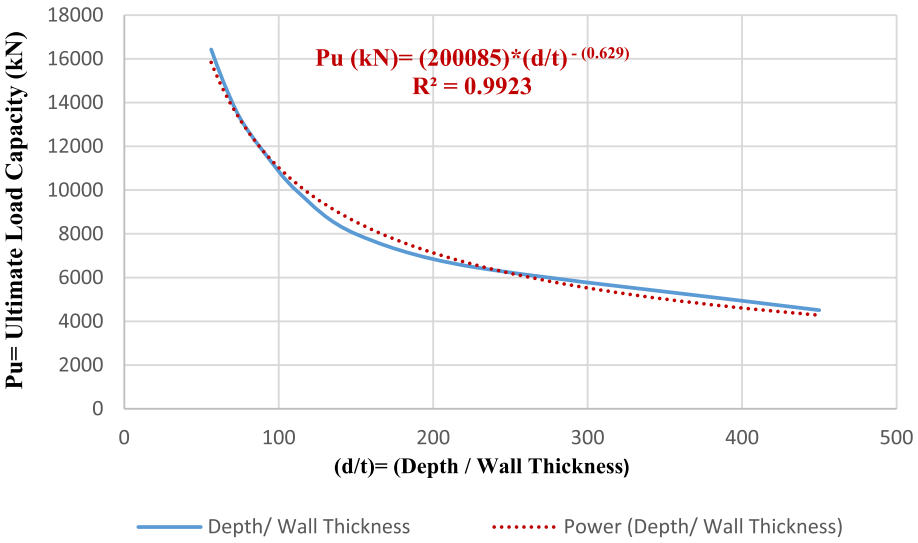

Fig. 27 T-shape LWCFST girder ultimate carrying load capacity

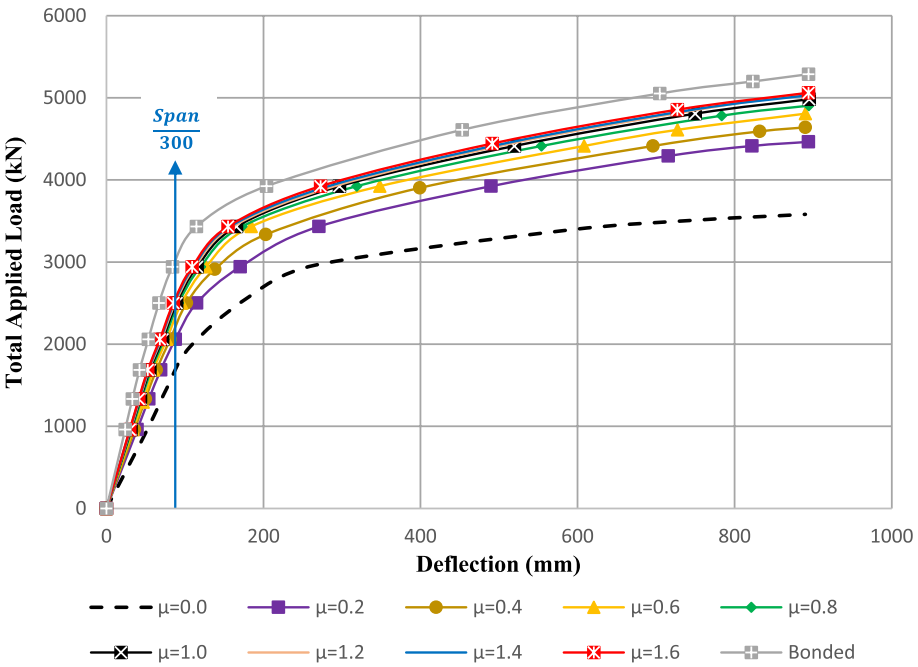

Fig. 28 Stiffness curves (μ)

$$K_{\text{Precast}} = K_{\text{Composite}} \tag{4}$$

$$\left(\frac{EI}{L}\right)_{\text{Precast.}} = \left(\frac{EI}{L}\right)_{\text{Steel Tube.}} + \left(\frac{EI}{L}\right)_{\text{Concrete}} \tag{5}$$

$$E_c = 4400\sqrt[2]{f_{Cu}}\ \left(N/mm^2\right) \tag{6}$$

Figure 25 shows that, increasing filler concrete f_{cu} increased the overall stiffness of the T-shape CFST girder, which in turn increases the area under the load–deflection curve leading to increasing the ductility, resilience, toughness, and the ultimate carrying load capacity of the T-shape CFST girder. Accordingly, enhancing the collapse scenario of the girder. Resilience was determined by integrating the area under the load–deflection curve up to the elastic limit, while toughness was determined by integrating the total area under the entire curve up to the plastic limit as shown in Figs. 29 and 30, respectively. Table 7 and Fig. 31 indicate the resilience, toughness, and ultimate carrying load capacity T-shape CFST girder corresponding to f_{cu} value.

Also, using 35 MPa filler concrete inside a 4-mm steel tube is enough to accomplish an equal stiffness to the precast girder. Meanwhile, its own weight is higher than the precast girders by 33.6%, with the same carrying load capacity.

The parametric study carried out on steel tube wall thickness (t_w) showed that using LWC inside a 16-mm steel tube accomplishes an equal stiffness to the precast girder as shown in Table 8. It is shown also that increasing steel tube wall thickness increased T-shape LWCFST girder stiffness. It leads to increasing both yielding and plastic limits, which in turn increases its ductility, resilience, toughness, and ultimate carrying load capacity. Accordingly, enhancing its collapse scenario is shown in Table 9 and Fig. 32.

The power equation deduced from Fig. 27 in terms of (d/t) and ultimate carrying capacity can be generally used for any value of (d/t) of the proposed T-shape LWCFST girder. Moreover, using 16mm wall thickness filled with lightweight concrete of 9MPa compressive strength and 0.65 specific density accomplishes an equal stiffness to the precast concrete girder. Meanwhile, its own weight is lighter than the precast girder by 20% with the same load capacity providing importance for using it in bridge construction.

Figure 28 shows that the rising friction coefficient value significantly affects the stiffness of T-shape LWCFST girder, but not at the same rate up to a friction coefficient of

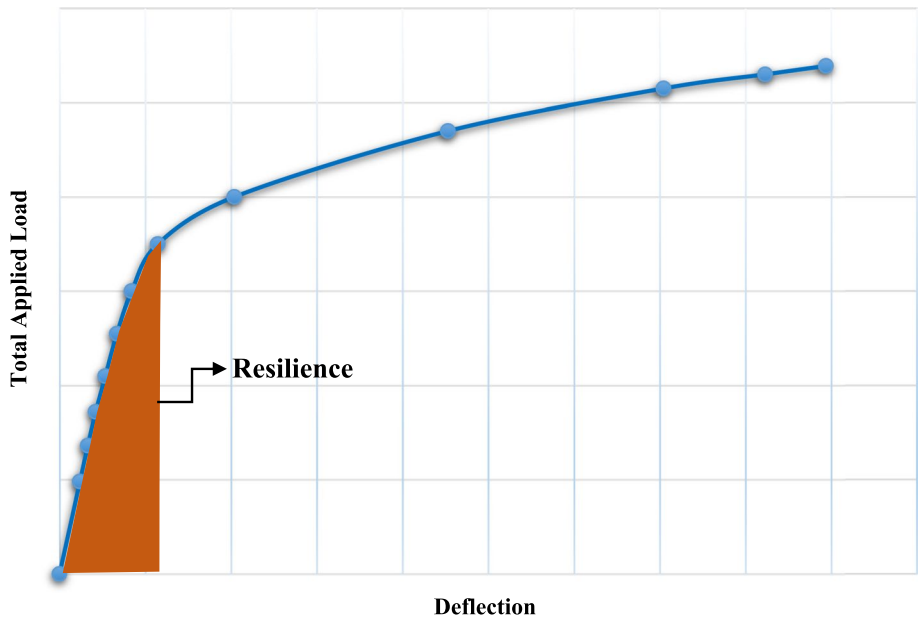

Fig. 29 Resilience of LWCFST girder

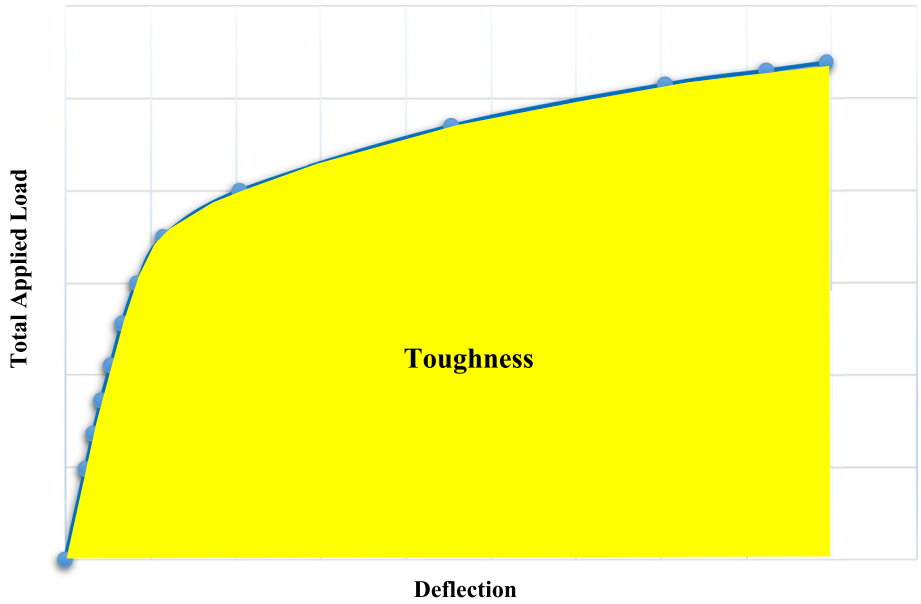

Fig. 30 Toughness of LWCFST girder

Table 7 Corresponding resilience, toughness, and ultimate load capacity to the filler concrete compressive strength (f_{cu})

$f_{cu}(MPa)$	**Resilience** ($kN.m.m^{-3}$)	**Toughness** ($kN.m.m^{-3}$)	**Ultimate carrying load capacity (kN)**
20	43.424	3665.798	5500
25	54.272	4581.573	6800
30	67.856	5728.317	8400
35	84.825	6450.860	10380
40	106.116	8070.02	12830
45	132.785	10098.172	13321
50	165.915	12617.677	14862

0.8. After this value, the stiffness of the T-shape LWCFST was slightly affected, no matter how high the friction coefficient is.

The parametric study carried out on the condition of the bond between steel tube and LWC clarified that, simulating the bond condition as a friction bond instead of a complete bond had a significant effect on T-shape LWCFST girder stiffness, ductility, resilience, toughness, and the ultimate carrying load capacity due to the variation of area under load–deflection curve. The bond physically behaves as a friction bond depending on the roughness value of the steel tube; hence, the resilience, toughness, and ultimate carrying load capacity in the case of friction bonding is less than complete bonding as shown in Table 10 and Fig. 33.

T-shape LWCFST girder failure criterion can be detailed in the yielding of steel tube lower flange at a tensile stress that exceeds 350 MPa (yield strength of steel-52), leading to cracking of the filler LWC. The crack width is increased directly, by increasing the applied load until the filler concrete is fully stressed with tension stresses. Meanwhile, the concrete of the upper flange crushes at compressive stress exceeding

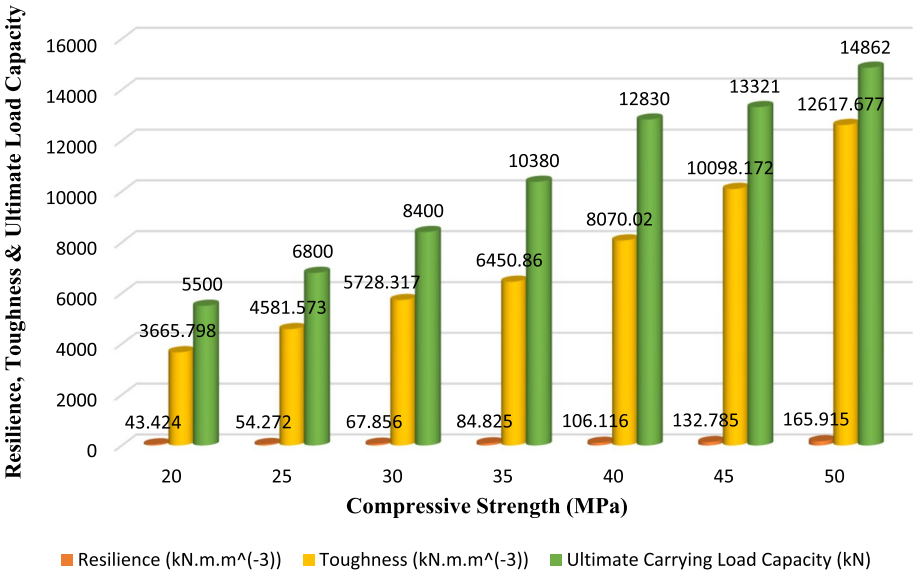

Fig. 31 (f_{cu}) resilience, toughness, and ultimate carrying load capacities

Table 8 Yielding and ultimate load capacity for precast and T-shape LWCFST girder

Capacity	Precast girder	T-shape LWCFST girder (16 mm) tube
Yield capacity (kN)	7500	7470
Ultimate capacity (kN)	9640	9670

Table 9 Corresponding resilience, toughness, and ultimate load capacity to steel tube wall thickness (t_w)

$t_w(mm)$	**Resilience** ($kN.m.m^{-3}$)	**Toughness** ($kN.m.m^{-3}$)	**Ultimate carrying load capacity (kN)**
4	37.98	3385.74	4750
8	47.42	4167.84	6018
12	59.20	5134.78	7625
16	73.905	6328.53	9670
20	92.25	7793.58	12240
24	115.22	9597.80	13293
28	143.85	11827.37	14930
32	179.51	14581.96	16432

50MPa (stopping criterion), which limits the ultimate load capacity of T-shape LWCFST girder as shown in Figs. 34, 35, 36, 37, 38, and 39. This failure criterion is steady for all performed parametric studies, but with different values of yielding and ultimate carrying load capacities. Table 8 illustrates the yielding and ultimate carrying load capacity for both precast concrete girder and T-shape LWCFST girder (16 mm tube thickness), which is the most appropriate T-shape LWCFST girder that can be used in bridge construction.

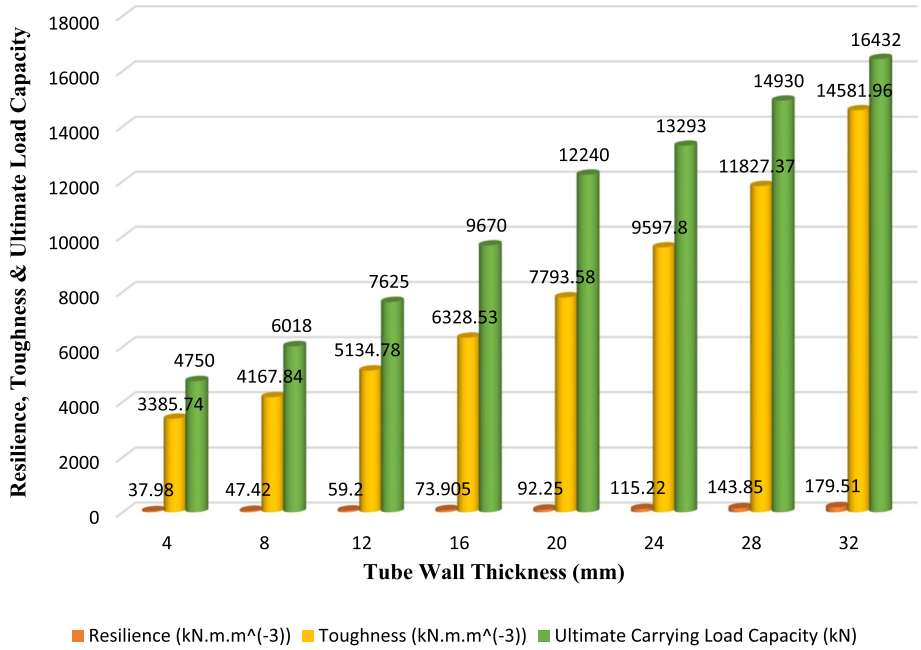

Fig. 32 (*tw*) resilience, toughness, and ultimate carrying load capacities

Table 10 Corresponding resilience, toughness, and ultimate load capacity to the bond condition

Bond condition	Resilience ($kN.m.m^{-3}$)	Toughness ($kN.m.m^{-3}$)	Ultimate carrying load capacity (kN)
Complete bond	47.42	3863.65	5288
Friction bond (μ = 0.8)	42.46	3524.80	4905

Lightweight concrete can be effectively used as a filler concrete because of its light self-weight. It was used only as a filler material and its significance is to delay the local web buckling of steel tube in order to increase its bending capacity [45], so its cracking and crack propagation weren't detailed in this study.

According to normal stress results illustrated in Figs. 34, 35, 36, 37, 38, and 39 for steel tube, LWC, and the concrete slab [46], the overall normal stress distribution for T-shape LWCFST girder at both yield and ultimate points can be represented in both Figs. 40 and 41 respectively.

Conclusions

In this research, a set of parameters was investigated on a proposed T-shape LWCFST girder to obtain an affordable, long-span, light-weight, and fast-constructing girder; in order to be used in bridge construction. Based on specifications and design codes (EN 1994–1-1/Euro code 4 and ANSI/AISC 360–10), the parameters considered were: the compressive strength of filler concrete f_{cu}, the wall thickness of steel tube (t_w) and the bond condition between the filler concrete and the steel tube (μ). According to the analysis results of these parameters, the following conclusions have been established as follow:

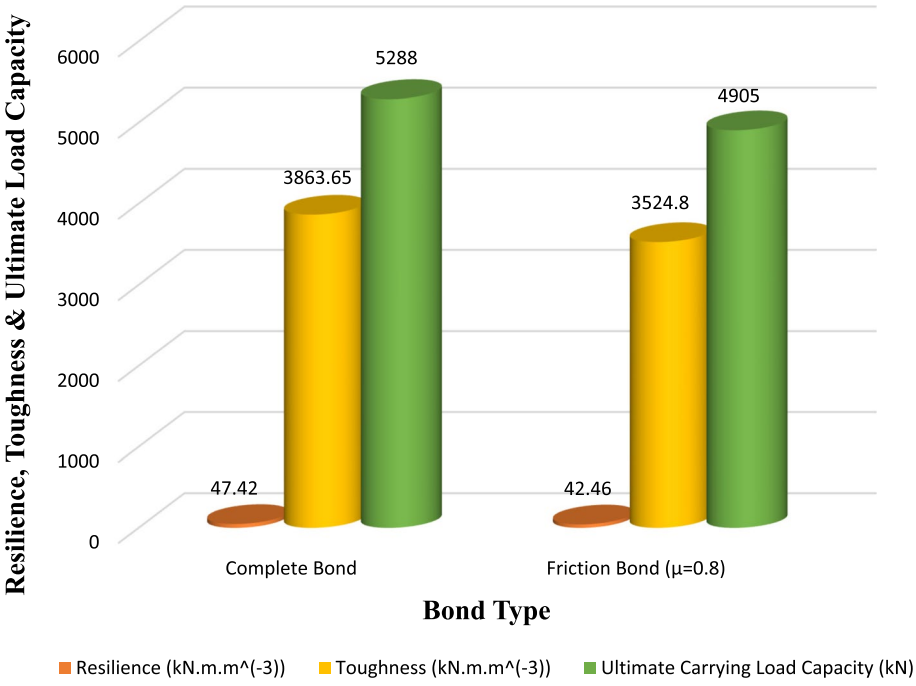

Fig. 33 (μ) resilience, toughness, and ultimate carrying load capacities

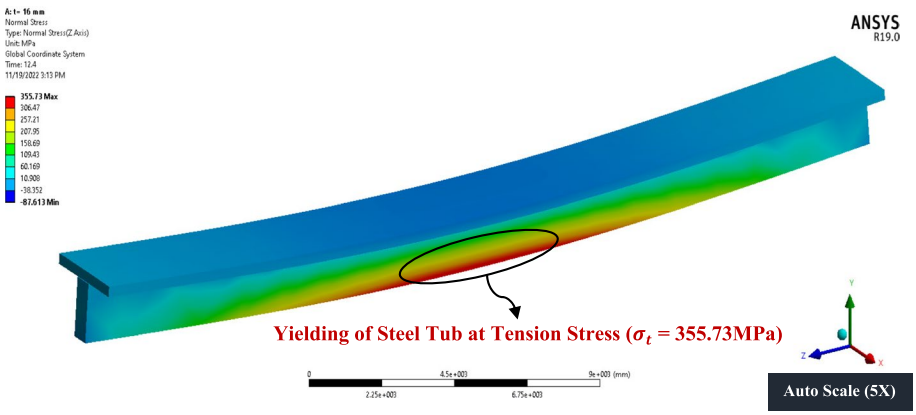

Fig. 34 Steel tube normal stress at yielding capacity

- Lightweight concrete can be effectively used as a filler concrete, which increased the carrying load capacity of T-shape LWCFST girder by 19% compared to the empty one.
- Increasing steel tube wall thickness for the current study by an increment of 4 mm using the same filler concrete leads to a constant increase in resilience, toughness, and carrying load capacity of T-shape LWCFST girder by 25%, 23%, and 26.7% respectively.
- It was found that increasing the compressive strength of filler concrete by 5 MPa increment through the current study within a range of 20 MPa to 50 MPa with the

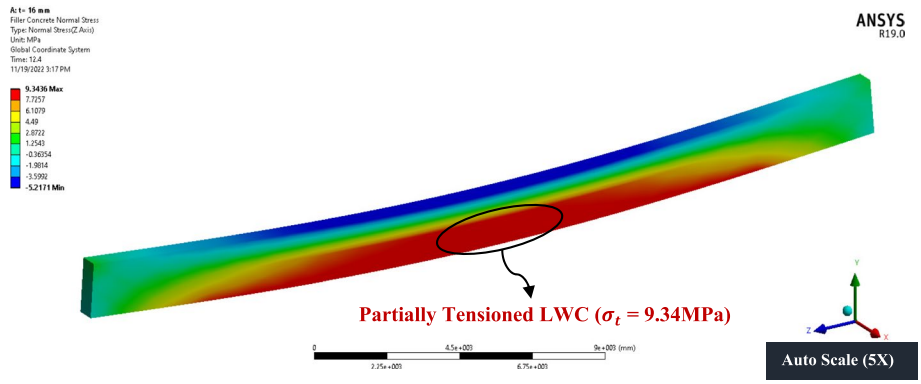

Fig. 35 LWC normal stress at yielding capacity

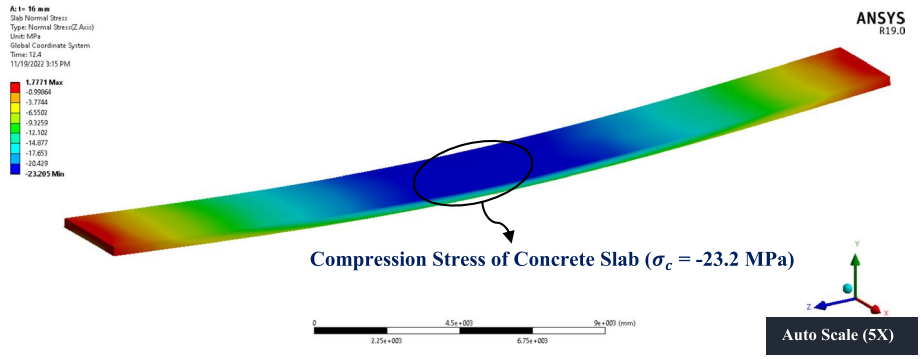

Fig. 36 Concrete slab normal stress at yielding capacity

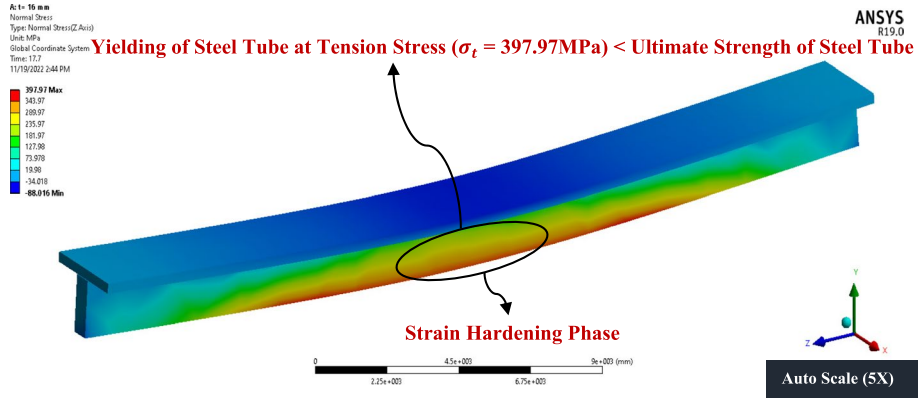

Fig. 37 Steel tube normal stress at ultimate capacity

same tube wall thickness, leads to a constant increase in resilience, toughness, and carrying load capacity of the CFST girder by 25%, 25%, and 23.6% respectively.

- The ultimate carrying load capacity of T-shape LWCFST girder filled with 9 MPa Compressive strength lightweight concrete can be determined in terms of (d/t) using the following power equation, taking into consideration it should meet the aforementioned dimensions described in this study [upper flange width (B_f

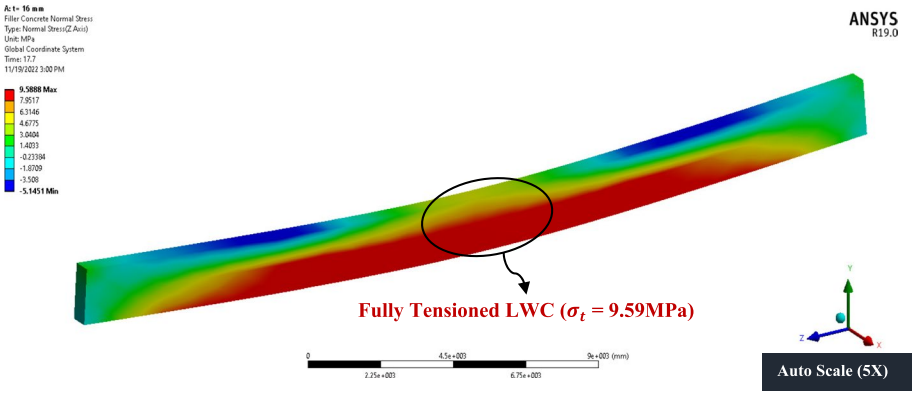

Fig. 38 LWC normal stress at ultimate capacity

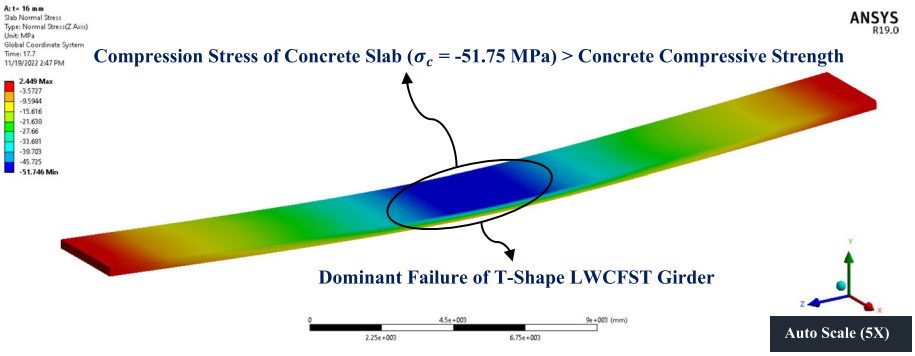

Fig. 39 Concrete slab normal stress at ultimate capacity

) = 2.80 m, upper flange thickness (t_f) = 0.20 m, steel tube width (b_t) = 0.65 m and steel tube depth (d_t) = 1.80 m].

$$P_u(kN) = (200085) * (d/t)^{-(0.629)}$$

This equation is valid for $P_u, d, t \in R$, where, $t > 0$ and $P_u \geq 0$.

- Applying a friction bond between lightweight concrete and steel tube with (μ = 0.8) instead of complete bonding, reduced the values of girder resilience, toughness, and ultimate carrying load capacity by 10.5%, 8.8%, and 7.2% respectively.
- Increasing the value of friction coefficient up to 0.8 was found to significantly affect the stiffness value, and has a slight effect after, no matter how high it is.
- The dominant failure of T-shape LWCFST girders was found in the upper concrete slab due to the compression stress, even though the tensile cracks in the filler concrete occurred after reaching tensile yield stress in the steel tube.
- It is concluded that T-shape LWCFST girders can be a significant relative economic alternative to precast girders in the bridge construction field due to their high stiffness/weight ratio.

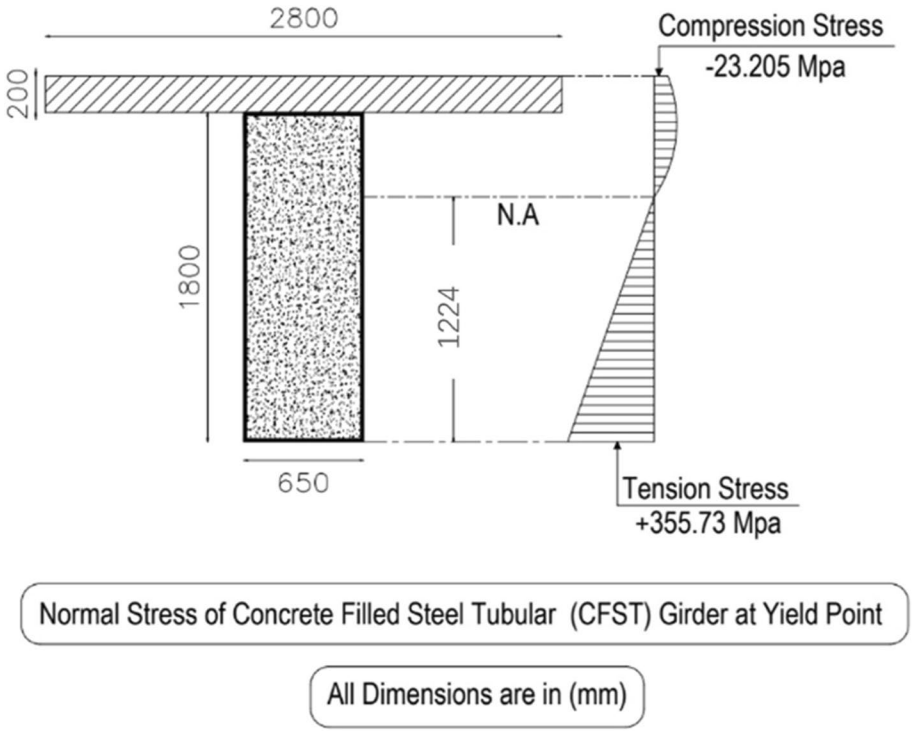

Fig. 40 T-shape LWCFST girders normal stress at yield point

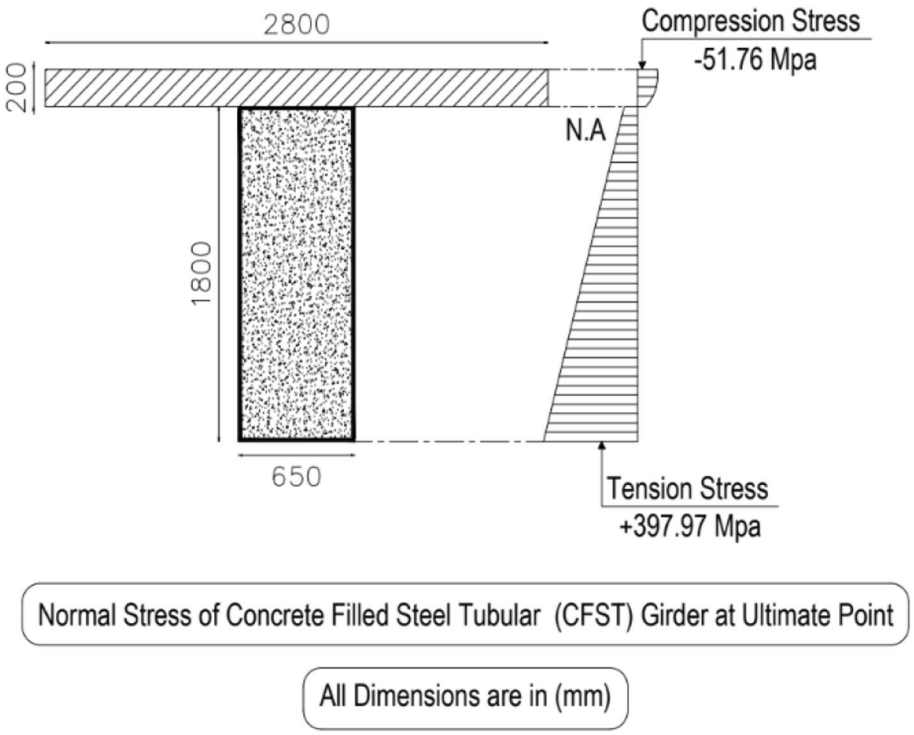

Fig. 41 T-shape LWCFST girder normal stress at the ultimate point

The conclusions of this research are limited to CFST girders filled with light-weight concrete. Further investigations are required using other filler concrete composites. So, the feasibility of using different filler concrete composites such as engineering cementitious composites (ECC) and fiber-reinforced concrete (FRC) with various types of fibers, can be conducted in future work.

Abbreviations

CFST	Concrete filled steel tube
CSA	Cored shell aggregate
DSM	Direct strength method
DOF	Degrees of freedom
FEM	Finite element model
FEA	Finite element analysis
LWC	Lightweight concrete
LWCFST	Lightweight concrete-filled steel tube
SCC	Self-compacted concrete
SCCST	Self-compacted concrete steel tube
FRC	Fiber reinforced concrete
f_{cu}	Cube compressive strength
f_{ck}^*	Characteristic cylinder compressive strength
f_{cr}^*	Concrete modulus of rupture/concrete tensile strength
f_{ct}^*	Concrete splitting tensile strength
μ	Friction coefficient
$\tilde{\sigma}$	Material stress
$\tilde{\varepsilon}$	Material strain
k'	Material strength coefficient
n	Material strain hardening exponent
E	Material Young's modulus
L	Member length
K	Member stiffness
I	Member moment of inertia
m	Strain rate sensitivity index
$\mathrm{t_w}$	Steel tube wall thickness
b_t	Steel tube width
d_t	Steel tube depth
B_f	Upper flange width
t_f	Upper concrete flange thickness

Acknowledgements
The authors are thankful to "Engineering Authority of the Egyptian Army" for providing all the necessary facilitation to carry out this research.

Authors' contributions
Each author has made substantial contributions to all aspects of preparing and writing this paper. Furthermore, each author has meticulously reviewed the manuscript and provided their unequivocal approval.

Funding
The authors received no financial support from any organization for the submitted work.

Availability of data and materials
The data generated and/or analyzed during this study are available upon reasonable request from the corresponding author.

Declarations

Competing interests
The authors declare that they have no competing interests.

Received: 18 September 2023 Accepted: 27 November 2023
Published online: 09 December 2023

References

1. Elshahawi M, Hückler A, Schlaich M (2021) Infra lightweight concrete: a decade of investigation (a review). Struct Concr 22(S1). https://doi.org/10.1002/suco.202000206

2. Bogas JA, Gomes MG, Gomes A (2013) Compressive strength evaluation of structural lightweight concrete by non-destructive ultrasonic pulse velocity method. Ultrasonics 53(5):962–972. https://doi.org/10.1016/j.ultras.2012.12.012
3. Bejan G, Bărbuță M, Ștefan Vizitiu R, Burlacu A (2020) Lightweight concrete with waste - review. Proc Manuf 46:136–143. https://doi.org/10.1016/j.promfg.2020.03.021
4. Yu QL, Spiesz P, Brouwers HJH (2015) Ultra-lightweight concrete: conceptual design and performance evaluation. Cem Concr Compos 61:18–28. https://doi.org/10.1016/j.cemconcomp.2015.04.012
5. Alduaij J, Alshaleh K, Haque MN, Ellaithy K (1999) Lightweight concrete in hot coastal areas. Cem Concr Compos 21(5–6):453–458. https://doi.org/10.1016/S0958-9465(99)00035-9
6. Chen B, Liu N (2013) A novel lightweight concrete-fabrication and its thermal and mechanical properties. Constr Build Mater 44:691–698. https://doi.org/10.1016/j.conbuildmat.2013.03.091
7. Vandanapu SN, Krishnamurthy M (2018) Seismic performance of lightweight concrete structures. Adv Civ Eng 2018:1–6. https://doi.org/10.1155/2018/2105784
8. Alqahtani FK, Abotaleb IS, ElMenshawy M (2021) Life cycle cost analysis of lightweight green concrete utilizing recycled plastic aggregates. J Build Eng 40:102670. https://doi.org/10.1016/j.jobe.2021.102670
9. Kurpinska M, Grzyl B, Kristowski A (2019) Cost analysis of prefabricated elements of the ordinary and lightweight concrete walls in residential construction. Materials 12(21):3629. https://doi.org/10.3390/ma12213629
10. Chanda SS, Patel SK, Nayak AN, Mohanty CR (2023) Performance evaluation on bond, durability, micro-structure, cost effectiveness and environmental impacts of fly ash cenosphere based structural lightweight concrete. Constr Build Mater 397:132429. https://doi.org/10.1016/j.conbuildmat.2023.132429
11. Mousa A, Mahgoub M, Hussein M (2018) Lightweight concrete in America: presence and challenges. Sustain Prod Consum 15:131–144. https://doi.org/10.1016/j.spc.2018.06.007
12. Ahmed IM, Tsavdaridis KD (2018) Life cycle assessment (LCA) and cost (LCC) studies of lightweight composite flooring systems. J Build Eng 20:624–633. https://doi.org/10.1016/j.jobe.2018.09.013
13. Mo KH, Alengaram UJ, Jumaat MZ (2016) Bond properties of lightweight concrete – a review. Constr Build Mater 112:478–496. https://doi.org/10.1016/j.conbuildmat.2016.02.125
14. Berthet JF, Yurtdas I, Delmas Y, Li A (2011) Evaluation of the adhesion resistance between steel and concrete by push out test. Int J Adhes Adhes 31:75–83. https://doi.org/10.1016/j.ijadhadh.2010.11.004
15. Campione G, Cucchiara C, Mendola LL, Papia M (2005) Steel–concrete bond in lightweight fiber reinforced concrete under monotonic and cyclic actions. Eng Struct 27(6):881–890. https://doi.org/10.1016/j.engstruct.2005.01.010
16. Bahrami A, Nematzadeh M (2021) Bond behavior of lightweight concrete-filled steel tubes containing rock wool waste after exposure to high temperatures. Constr Build Mater 300:124039. https://doi.org/10.1016/j.conbuildmat.2021.124039
17. Sikora P, Rucinska T, Stephan D, Chung S-Y, Abd Elrahman M (2020) Evaluating the effects of nanosilica on the material properties of lightweight and ultra-lightweight concrete using image-based approaches. Constr Build Mater 264:120241. https://doi.org/10.1016/j.conbuildmat.2020.120241
18. Chung S-Y, Elrahman MA, Stephan D, Kamm PH (2018) The influence of different concrete additions on the properties of lightweight concrete evaluated using experimental and numerical approaches. Constr Build Mater 189:314–322. https://doi.org/10.1016/j.conbuildmat.2018.08.189
19. Tajra F, Elrahman MA, Lehmann C, Stephan D (2019) Properties of lightweight concrete made with core-shell structured lightweight aggregate. Constr Build Mater 205:39–51. https://doi.org/10.1016/j.conbuildmat.2019.01.194
20. Al-Shaar AAM, Göğüş MT (2018) Flexural behavior of lightweight concrete and self-compacting concrete-filled steel tube beams. J Constr Steel Res 149:153–164. https://doi.org/10.1016/j.jcsr.2018.07.027
21. AISC Committee (2010) Specification for structural steel buildings (ANSI/AISC 360–10). American Institute of Steel Construction, Chicago
22. Johnson RP, Anderson D (2004) Designers' guide to EN 1994-1-1: eurocode 4: design of composite steel and concrete structures. Part 1.1: General rules and rules for buildings. London, Thomas Telford
23. DBJ 13-51-2010 (2010). Design method of technical specification for concrete-filled steel tubular, DBJ 13-51-2010, Fujian Provincial Construction Department, Fuzhou, China.
24. Australian Standards, AS5100.2 (2004), 'Bridge design - Part 2: Design loads, Standards Australia international Ltd.
25. Architectural Institute of Japan (1987) Standards for structural calculation of steel reinforced concrete structures
26. Liew JYR, Sohel KMA, Koh CG (2009) Impact tests on steel–concrete–steel sandwich beams with lightweight concrete core. Eng Struct 31(9):2045–2059. https://doi.org/10.1016/j.engstruct.2009.03.007
27. Sifan M, Gatheeshgar P, Nagaratnam B, Poologanathan K, Navaratnam S, Thamboo J, Corradi M (2022) Flexural behaviour and design of hollow flange cold-formed steel beam filled with lightweight normal and lightweight high strength concrete. J Build Eng 48:103878. https://doi.org/10.1016/j.jobe.2021.103878
28. Gulec A, Kose MM, Gogus MT (2020) An analysis of the usability of prefabricated cage-reinforced composite beams with self-compacting and lightweight concrete under flexural loads. Constr Build Mater 255:119274. https://doi.org/10.1016/j.conbuildmat.2020.119274
29. Sifan M, Gatheeshgar P, Nagaratnam B, Poologanathan K, Navaratnam S, Thamboo J, Suntharalingam TH (2022) Shear performance of lightweight concrete filled hollow flange cold-formed steel beams. Case Stud Constr Mater 17:e01160. https://doi.org/10.1016/j.cscm.2022.e01160
30. Uenaka K, Mizukoshi M (2021) Lightweight concrete filled steel tubular beam under bending-shear. Structures 30:659–666. https://doi.org/10.1016/j.istruc.2020.12.072
31. Al-Eliwi BJ, Ekmekyapar T, Al-Samaraie MI, Doğru MH (2018) Behavior of reinforced lightweight aggregate concrete-filled circular steel tube columns under axial loading. Structures 16:101–111. https://doi.org/10.1016/j.istruc.2018.09.001
32. Ghannam S (2016) Flexural strength of concrete-filled steel tubular beam with partial of coarse aggregate by granite. IAEME Publ 7(5):161–168. ISSN Online: 0976-6316, ISSN Print: 0976-6308, https://iaeme.com/Home/article_id/IJCIET_07_05_018
33. Al Zand AW, Alghaaeb MF, Liejy MC, Mutalib AA, Al-Ameri R (2022) Stiffening performance of cold-formed c-section beam filled with lightweight-recycled concrete mixture. Materials 15(9):2982. https://doi.org/10.3390/ma15092982

34. Hambly EC (1991) Bridge deck behavior, 2nd edn. British Library Cataloguing in Publication Data. Boca Raton, CRC press
35. Voyiadjis GZ, Yaghoobi M (2019) Nonlocal crystal plasticity. In Size effects in plasticity - chapter 3. Elsevier. Cambridge, Academic press. p 191–232. https://doi.org/10.1016/B978-0-12-812236-5.00003-7
36. Aghaie-Khafri M, Mahmudi R, Pishbin H (2002) Role of yield criteria and hardening laws in the prediction of forming limit diagrams. Metall Mater Trans A 33(5):1363–1371. https://doi.org/10.1007/s11661-002-0061-1
37. Dolati A, Maleki S (2019) Ductile behavior of existing internal end diaphragms in steel tub girder bridges. J Constr Steel Res 153:356–371. https://doi.org/10.1016/j.jcsr.2018.10.019
38. Gajewski MD, Miecznikowski M (2021) Assessment of the suitability of elastomeric bearings modeling using the hyper-elasticity and the finite element method. Materials 14(24):7665. https://doi.org/10.3390/ma14247665
39. Guo Q, Chen Q, Xing Y, Xu Y, Zhu Y (2020) Experimental study of friction resistance between steel and concrete in prefabricated composite beam with high-strength frictional bolt. Adv Mater Sci Eng 2020:1–13. https://doi.org/10.1155/2020/1292513
40. Wang F-C, Xie W-Q, Li B, Han L-H (2022) Experimental study and design of bond behavior in concrete-filled steel tubes (CFST), Elsevier. Eng Struct 268:114750. https://doi.org/10.1016/j.engstruct.2022.114750
41. Shivadarshan S, Kumar C, Kumar NS (2019) Experimental investigation on bond strength in self-compacting concrete filled steel tube. Int Res J Eng Technol 6(7)
42. Tao M-X, Li Z-A, Zhou Q-L, Xu L-Y (2021) Analysis of equivalent flexural stiffness of steel–concrete composite beams in frame structures. Appl Sci 11(21):10305. https://doi.org/10.3390/app112110305
43. Liang QQ (2009) Performance-based analysis of concrete-filled steel tubular beam–columns, Part I: theory and algorithms, Elsevier. J Constr Steel Res 65(2):363–372. https://doi.org/10.1016/j.jcsr.2008.03.007
44. Tao Z, Han L-H (2006) Behavior of concrete-filled double skin rectangular steel tubular beam–columns, Elsevier. J Constr Steel Res 62(7):631–646. https://doi.org/10.1016/j.jcsr.2005.11.008
45. Thienel KC, Haller T, Beuntner N (2020) Lightweight concrete—from basics to innovations. Materials 13(5):1120. https://doi.org/10.3390/ma13051120
46. ANSYS, Inc. and ANSYS Europe, Ltd. ANSYS Workbench Release 19.0. http://www.ansys.com. Accessed May 2023.

Publisher's Note